11655

# Using Structures Formed by Dirhodium Tetra(trifluoroacetate) with Polycyclic Aromatic Hydrocarbons to Prospect for Maximum π-Electron Density: Hückel Calculations Get It Right

**F. Albert Cotton,\*,† Evgeny V. Dikarev,†,‡ and Marina A. Petrukhina†,‡**

*Contribution from the Laboratory for Molecular Structure and Bonding, Department of Chemistry, Texas A&M University, P.O. Box 30012, College Station, Texas 77842-3012*

*Received August 9, 2001*

**Abstract:** A new class of supramolecular assemblies derived from a powerful Lewis acid in the form of dirhodium(II) tetra(trifluoroacetate) and various planar polycyclic aromatic hydrocarbons (PAHs) as donors has been prepared using a solventless technique. As a result, a number of novel adducts $[Rh_2(O_2CCF_3)_4]_x(L)_y$ with various stoichiometries, $x{:}y = 1{:}2$, 1:1, 3:2, and 3:1, have been isolated in crystalline form. The following PAHs have been employed: acenaphthylene $C_{12}H_8$ (**L1**); acenaphthene $C_{12}H_{10}$ (**L2**); anthracene (**L3**) and phenanthrene (**L4**), $C_{14}H_{10}$; pyrene (**L5**) and fluoranthene (**L6**), $C_{16}H_{10}$; a series of isomers of the $C_{18}H_{12}$ composition: 1,2-benzanthracene (**L7**), triphenylene (**L8**), and chrysene (**L9**). Single-crystal X-ray diffraction studies have revealed a variety of structural motifs ranging from discrete molecules to extended 1D chains and 2D networks. In the bis-adducts, $[Rh_2(O_2CCF_3)_4](L)_2$, an aromatic ligand is axially coordinated to the rhodium atoms through two long inequivalent Rh−C linkages at each end of the dirhodium complex. In the 1D complexes $\{[Rh_2(O_2CCF_3)_4](L)\}_\infty$ aromatic ligands serve as bidentate links between two dirhodium units, while in 2D structures PAHs act as polydentate linkers, each coordinated to several rhodium atoms. Each linkage of a PAH consisted of an off-centered $\eta^2$ coordination toward a single rhodium center. Simple Hückel calculations performed on the PAHs were used to calculate π-electron densities for the C−C bonds, and these densities were compared to the experimental results.

## Introduction

Polycyclic aromatic hydrocarbons (PAHs) have attracted considerable attention in materials science due to their shapes and other properties arising from their extended delocalized π-systems.[1] While it is well-known that single-ring aromatic ligands form π-complexes with a variety of electron-deficient molecules,[2] multiring arenes have only recently been investigated as potential ligands for the preparation of donor−acceptor materials.[3] In particular, incorporation of transition metal centers into PAH systems was found to have a dramatic influence on the reactivity of the solid surfaces[4] and resulted in potential applications as electrical conductors[5] and photosensitive devices.[6] Despite these achievements, it could be said that the potential of PAHs for building macromolecular structures and hybrid materials with transition metals has not been fully explored.

Recently, we began exploring the extraordinary Lewis acidity of dirhodium(II) tetra(trifluoroacetate), $Rh_2(O_2CCF_3)_4$,[7] by means of a methodology we call solventless synthesis.[8] This work was prompted by the following facts.

First, $Rh_2(O_2CCF_3)_4$ is an extremely strong Lewis acid.

Second, it has two sites of Lewis acidity rigidly oriented in space; it is not only a bifunctional Lewis acid, which can serve as a linker between two donors, but it also dictates their spacial relationship.

Third, because it is such a powerful Lewis acid, it is difficult to obtain adducts with weak Lewis bases by conventional

* Address correspondence to this author. E-mail: cotton@tamu.edu.
† Texas A&M University.
‡ State University of New York at Albany.

(1) (a) Debad, J. D.; Morris, J. C.; Lynch, V.; Magnus, P.; Bard, A. J. *J. Am. Chem. Soc.* **1996**, *118*, 2374−2379. (b) Ohashi, K.; Kubo, T.; Masui, T.; Yamamoto, K.; Nakasuji, K.; Takui, T.; Kai, Y.; Murata, I. *J. Am. Chem. Soc.* **1998**, *120*, 2018−2027. (c) Harvey, R. G. *Polycyclic Aromatic Hydrocarbons*; Wiley-VCH: New York, 1997. (d) Kübel, C.; Eckhardt, K.; Enkelmann, V.; Wegner, G.; Müllen, K. *J. Mater. Chem.* **2000**, *10*, 879−886. (e) Sygula, A.; Rabideau, P. W. *J. Am. Chem. Soc.* **2000**, *122*, 6323−6324.

(2) (a) Mecozzi, S.; West, A. P.; Dougherty, D. A. *J. Am. Chem. Soc.* **1996**, *118*, 2307−2308. (b) Dougherty, D. A. *Science* **1996**, *271*, 163−168. (c) Evans, D. R.; Fackler, N. L. P.; Xie, Z.; Rickard, C. E. F.; Boyd, P. D. W.; Reed, C. A. *J. Am. Chem. Soc.* **1999**, *121*, 8466−8474. (d) Tsuzuki, S.; Honda, K.; Uchimaru, T.; Mikami, M.; Tanabe, K. *J. Am. Chem. Soc.* **2000**, *122*, 3746−3753. (e) Tarakeshwar, P.; Kim, K. S. *J. Phys. Chem. B* **1999**, *103*, 9116−9124.

(3) (a) Krygowski, T. M.; Ciesielski, A.; Swirska, B.; Leszczynski, P. *Polish J. Chem.* **1994**, *68*, 2097−2107. (b) Vezzosi, I. M.; Zanoli, A. F.; Battaglia, L. P.; Corradi, A. B. *J. Chem. Soc., Dalton Trans.* **1988**, 191−193. (c) Battaglia, L. P.; Bellitto, C.; Cramarossa, M. R.; Vezzosi, I. M. *Inorg. Chem.* **1996**, *35*, 2390−2392. (d) Aoyama, Y.; Endo, K.; Anzai, T.; Yamaguchi, Y.; Sawaki, T.; Kobayashi, K.; Kanehisa, N.; Hashimoto, H.; Kai, Y.; Masuda, H. *J. Am. Chem. Soc.* **1996**, *118*, 5562−5571.

(4) (a) Hasegawa, T.; Sekine, M.; Schaefer, W. P.; Taube, H. *Inorg. Chem.* **1991**, *30*, 449−452. (b) Rabaa, H.; Lacoste, M.; Delvill-Desbois, M. H.; Ruiz, J.; Gloaguen, B.; Ardoin, N.; Astruc, D.; Le Beuze, A.; Saillard, J.-Y.; Linares, J.; Varret, F.; Dance, J.-M.; Marquestaut, E. *Organometallics* **1995**, *14*, 5078−5092. (c) Elschenbroich, C.; Möckel, R.; Vasil'kov, A.; Metz, B.; Harms, K. *Eur. J. Inorg. Chem.* **1998**, 1391−1401.

(5) Sergeev, G.; Zagorsky, V.; Petrukhina, M.; Zav'jalov, S.; Grigor'ev, E.; Trakhtenberg, L. *Anal. Commun.* **1997**, *34*, 113−114.

(6) Tanaka, H.; Tokito, S.; Taga, Y.; Okada, A. *J. Mater. Chem.* **1998**, *8*, 1999−2003.

(7) (a) Johnson, S. A.; Hunt, H. R.; Newman, H. M. *Inorg. Chem.* **1963**, *2*, 960−962. (b) Felthouse, T. R. *Progr. Inorg. Chem.* **1982**, *29*, 73−166. (c) Cotton, F. A.; Falvello, L. R.; Gerards, M.; Snatzke, G. *J. Am. Chem. Soc.* **1990**, *112*, 8979−8980. (d) Cotton, F. A.; Dikarev, E. V.; Feng, X. *Inorg. Chim. Acta* **1995**, *237*, 19−26. (e) Lichtenberger, D. L.; Pollard, J. R.; Lynn, M. A.; Cotton, F. A.; Feng, X. *J. Am. Chem. Soc.* **2000**, *122*, 3182−3190.

**Scheme 1**



$R_6 = H_6, H_4Me_2, Me_6$
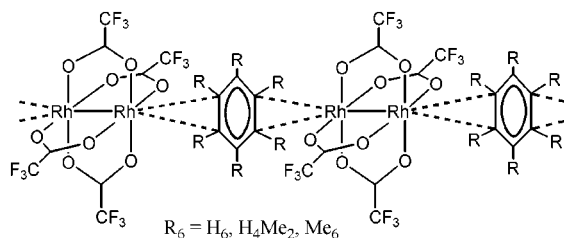
solution methods, since in general solvents for $Rh_2(O_2CCF_3)_4$ are themselves fairly good electron donors and thus preclude the binding of weaker donors.
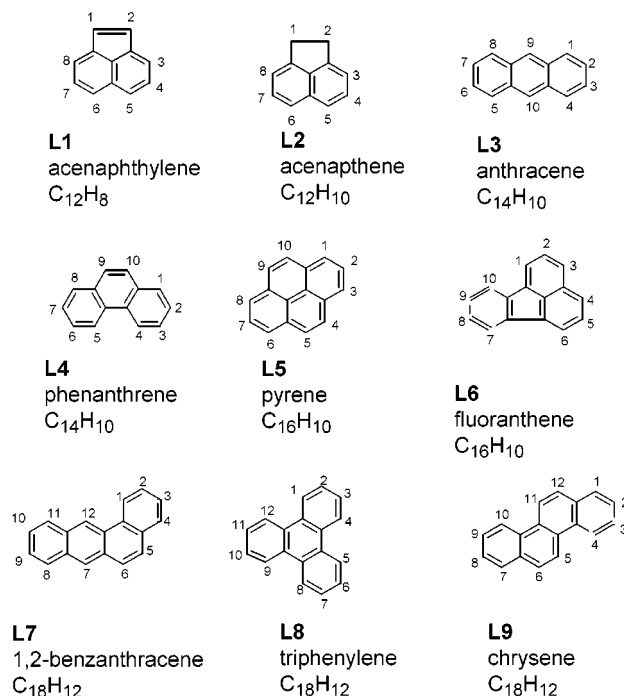
Fourth, however, $Rh_2(O_2CCF_3)_4$ is volatile, subliming rapidly at moderate temperatures (ca. 250 °C), and thus reactions can be conducted without solvent, by sublimation–deposition procedures from the gas phase.

This solventless approach opens unique opportunities to study interactions which are unobservable in solutions because solvent competition with weak donors as well as other solvent influences on the reaction pathway are completely excluded. Under the novel conditions of the solventless procedure we have already tested reactions of $Rh_2(O_2CCF_3)_4$ with numerous ligands, ranging from strong σ-donors to extremely weak donor molecules. Among these have been the π-arene ligands benzene,[8f] hexamethylbenzene,[8a] *p*-xylene,[8f] naphthalene,[8f] and diphenylacetylene.[8d] The binding of single-ring arene ligands by the dirhodium units occurred in each case through the approach of adjacent pairs of carbon atoms to each Rh atom (Scheme 1) to form chain (1D) polymers with aromatic bridges in the $\mu^2$-$\eta^2$: $\eta^2$ coordination mode. In the case of naphthalene one C−C pair in each ring approached a metal atom.

In view of the results obtained with monocyclic donors and naphthalene, we undertook the logical extension to other polycyclic aromatic systems which we expected would lead to more complex structures with higher $Rh_2$ to aromatic ligand ratios. We present here results of a systematic investigation of reactions of $Rh_2(O_2CCF_3)_4$ with the following polycyclic aromatic hydrocarbons (PAHs): acenaphthylene, $C_{12}H_8$ (**L1**); acenaphthene, $C_{12}H_{10}$ (**L2**); anthracene (**L3**) and phenanthrene (**L4**), $C_{14}H_{10}$; pyrene (**L5**) and fluoranthene (**L6**), $C_{16}H_{10}$; as well as with a series of isomers of the $C_{18}H_{12}$ composition: 1,2-benzanthracene (**L7**), triphenylene (**L8**), and chrysene (**L9**) (Scheme 2). Because of the overall planarity of their structures and the extended delocalized π-systems, featuring various shapes and sizes, as well as potential multisite coordination possibilities, these ligands seemed very promising for the construction of new extended solid materials with incorporated dinuclear transition metal units.

We can now report the structures of 13 novel products having $Rh_2(O_2CCF_3)_4$ and various PAHs as molecular components. They vary from discrete molecules to one- and two-dimensional extended networks. In each case the modes of attachment of the PAHs can be correlated with their π-electron distribution as given by Hückel π-molecular orbital theory. Thus, the Hückel

(8) (a) Cotton, F. A.; Dikarev, E. V.; Stiriba, S.-E. *Organometallics* **1999**, *18*, 2724−2726. (b) Cotton, F. A.; Dikarev, E. V.; Stiriba, S.-E. *Inorg. Chem.* **1999**, 38, 4877−4881. (c) Cotton, F. A.; Dikarev, E. V.; Petrukhina, M. A. *J. Organomet. Chem.* **2000**, *596*, 130−135. (d) Cotton, F. A.; Dikarev, E. V.; Petrukhina, M. A.; Stiriba, S.-E. *Organometallics* **2000**, *19*, 1402−1405. (e) Cotton, F. A.; Dikarev, E. V.; Petrukhina, M. A. *Angew. Chem., Int. Ed.* **2000**, *39*, 2362−2365. (f) Cotton, F. A.; Dikarev, E. V.; Petrukhina, M. A.; Stiriba, S.-E. *Polyhedron* **2000**, *19*, 1829−1835. (g) Cotton, F. A.; Dikarev, E. V.; Petrukhina, M. A. *Angew. Chem., Int. Ed.* **2001**, *40*, 1521−1523.

**Scheme 2**



**L1**
acenaphthylene
$C_{12}H_8$

**L2**
acenapthene
$C_{12}H_{10}$

**L3**
anthracene
$C_{14}H_{10}$

**L4**
phenanthrene
$C_{14}H_{10}$

**L5**
pyrene
$C_{16}H_{10}$

**L6**
fluoranthene
$C_{16}H_{10}$

**L7**
1,2-benzanthracene
$C_{18}H_{12}$

**L8**
triphenylene
$C_{18}H_{12}$

**L9**
chrysene
$C_{18}H_{12}$

calculations serve as a reliable basis for understanding the construction of solid-state materials with desired architectures.

The topics covered in this contribution are grouped into the following sections: (a) the fundamentals of the solventless technique and stoichiometric control of the synthesis of various adducts, (b) structural descriptions and discussion of the coordination modes of the PAHs, (c) Hückel calculations as a basis for anticipation of the preferential binding sites of PAHs by the rhodium centers.

## Experimental Section

**General Information**. All synthetic manipulations were carried out under an atmosphere of dry, oxygen-free dinitrogen by employing Schlenk techniques. The unligated form of $Rh_2(O_2CCF_3)_4$ was prepared using a literature procedure.[7d] All aromatic ligands were purchased from Aldrich and recrystallized by sublimation prior to use. The EI/DP mass spectra were acquired at 10−70 eV using a VG Analytical 70S high-resolution, double focusing sectored (EB) mass spectrometer. Elemental analyses were done by Canadian Microanalytical Services, Ltd. The IR spectra were performed on a Perkin-Elmer 16PC FT-IR spectrophotometer using KBr pellets.

**Synthesis of $[Rh_2(O_2CCF_3)_4]_x(L)_y$ Adducts**. Unligated solid dirhodium(II) tetra(trifluoroacetate), $Rh_2(O_2CCF_3)_4$, was prepared[7d] with special precautions to avoid even traces of any coordinated solvent: water, acetone, and so forth. All PAH ligands (**L1**−**L9**) used are presented in Scheme 2 along with the names, compositions, and abbreviations.

In a typical experiment unligated $Rh_2(O_2CCF_3)_4$ (0.066 g, 0.10 mmol) was mixed with a freshly sublimed aromatic ligand (**L1**−**L9**) at an appropriate ratio under a dinitrogen atmosphere. The mixture was sealed in an evacuated Pyrex tube, and the tube was placed in an electric furnace at the given temperature. After some period of time crystals of products were deposited on the walls of the tube, predominantly in its "cold" zone, where the temperature was set about 5 °C lower. The initial experimental conditions for the various reactions and some results for PAHs **L1**−**L9** are summarized in Table 1.

**X-ray Crystallographic Procedures**. Single crystals of the products were obtained as described above. The X-ray diffraction experiments were carried out on a Nonius FAST diffractometer with an area detector using Mo Kα radiation. In each case, a crystal of suitable quality was affixed to the end of a quartz fiber with grease in a cold nitrogen stream

**Table 1.** Experimental Synthetic Details for Preparations of the Adducts **1**−**9**

| ligand | $T_{melt}$ (°C) | Rh₂:L (initial) | temp (°C) | time (days) | zone[a] | Rh₂:L (product) | yield (%) | crystal description | product |
|---|---|---|---|---|---|---|---|---|---|
| **L1** | 90−92 | 1:0.6 | 110−120 | 3 | cold | 1:1 | 25−30 | blocks | **1b** |
| acenaphthylene | | 1:1 | 120 | 10 | cold | 1:1 | 35 | blocks | **1b** |
| | | 1:1.3 | 145 | 7 | cold | 1:1 | 40−45 | blocks | **1b**[b] |
| **L2** | 93−95 | 1:1.3 | 100 | 3 | cold | 1:1 | 20 | cubes | **2b** |
| acenaphthene | | 1:1 | 135 | 10 | cold | 1:1 | 30 | cubes | **2b** |
| **L3** | 216−218 | 1:1 | 165 | 2 | cold/hot | 1:1 | 35 | rhombs | **3b** |
| anthracene | | 1:0.9 | 165 | 7 | cold | 1:1 | 45 | rhombs | **3b** |
| **L4** | 99−101 | 1:1 | 120−125 | 5 | cold | 1:1 | 30 | blocks | **4b** |
| phenanthrene | | 1:1 | 110 | 15 | cold | 1:1 | 45 | blocks | **4b** |
| **L5** | 150 | 1:1.25 | 135 | 11 | hot | 1:1 | 15 | needles | **5b** |
| pyrene | | 1:1 | 150 | 20 | hot | 1:1 | 25 | needles | **5b** |
| **L6** | 109−111 | 1:1.5 | 100 | 4 | cold | 1:2 | 30 | blocks | **6a** |
| fluoranthene | | 1:1 ⎱ | 105 | 2 | cold | 1:2 | 15 | blocks | **6a**[c] |
| | | 1:1 ⎰ | 105 | 2 | hot | 1:1 | 35−40 | needles | **6b**[c] |
| | | 1:1 | 160 | 4 | cold | 1:1 | 55 | needles | **6b′**[d] |
| **L7** | 157−159 | 1:1 | 180 | 3 | hot | 1:1 | 15 | needles | **7b** |
| 1,2-benzanthracene | | 1:1 | 190 | 10 | hot | 1:1 | 25 | needles | **7b** |
| **L8** | 197−200 | 1:2 | 140 | 3 | cold | 1:2 | 35 | cubes | **8a** |
| triphenylene | | 1:0.9 ⎱ | 140 | 2 | cold | 1:2 | 20 | cubes | **8a**[e] |
| | | 1:0.9 ⎰ | 140 | 2 | hot | 3:2 | 30 | tiny blocks | **8c**[e] |
| | | 1:0.75 | 150 | 5 | hot | 3:2 | 35 | tiny blocks | **8c** |
| **L9** | 252−254 | 1:1.3 | 160 | 10 | cold | 1:1 | 40−45 | needles | **9b** |
| chrysene | | 1:1.5 | 160 | 5 | cold | 1:1 | 35 | needles | **9b** |
| | | 1:0.75 | 180 | 4 | hot | 3:1 | 15 | plates | **9c** |
| | | 1:0.8 | 180 | 7 | hot | 3:1 | 20 | plates | **9c** |

[a] Location of the crystals in the ampule. [b] One crystal of **2b** was found mixed with crystals of **1b**. [c] Mixture of products. [d] **6b′** another polymorph 1:1. [e] Mixture of products

(−60 °C). Unit cell determination and data collection followed routine procedures and practices of this laboratory.[7c,8c] Oscillation photographs of principal axes were taken to confirm the Laue class and axial lengths. All data were corrected for Lorentz and polarization effects. The structures were solved and refined using the SHELXTL direct methods[9] and the SHELXL-93 programs[10] on a DEC Alpha running VMS. The fluorine atoms of all CF₃ groups were found to be disordered over two or three different rotational orientations. That disorder was modeled in each case. Anisotropic displacement parameters were assigned to all non-hydrogen atoms except the disordered fluorine atoms. For the structures **8c** and **9c**, because of a poor ratio of the number of reflections to the number of parameters, only Rh and O atoms were refined anisotropically. In each model, the hydrogen atoms were included in the structure factor calculations at idealized positions. Relevant crystallographic data for all the compounds are summarized in Table 2.

## Results

**Preparation of the [Rh₂(O₂CCF₃)₄]$_x$(L)$_y$ Adducts**. The synthetic approach based on the sublimation−deposition of the volatile Lewis acid, dirhodium(II) tetra(trifluoroacetate), in the presence of various PAHs led to the remarkable family of adducts of various compositions [Rh₂(O₂CCF₃)₄]$_x$(L)$_y$. For nine ligands chosen at the initial investigation stage (**L1**−**L9**), 13 new donor−acceptor products listed in Table 1 with the appropriate numbering have been obtained. All of them are green crystalline materials which have been isolated in a pure form. They are relatively stable in air at ambient conditions, but show some moisture sensitivity. Chemical analyses have been performed for all products except **5b** and **7b** to confirm their compositions (see Supporting Information); four different stoichiometries have been found. The results for two adducts **6a** and **8a** were consistent with the ratio Rh₂:L = 1:2 characteristic for bis-adduct type molecules; nine products had the composition

(9) *SHELXTL*, V.5; Siemens Industrial Automation Inc.: Madison, WI, 1994.
(10) Sheldrick, G. M. In *Crystallographic Computing 6*; Falck, H. D., Parkanyi, L., Simon, K., Eds.; Oxford University Press: Oxford, 1993; p 111.

of 1:1, while the two products **8c** and **9c** clearly exhibited the ratio of Rh₂ to L higher than that of a monoadduct, 3:2 and 3:1, respectively.

The solid injection technique of EI mass spectroscopy applied to crystals of adducts of various compositions always indicated an immediate cleavage of arenes from the products as only [Rh₂(O₂CCF₃)$_n$]⁺ ($n = 1$−4) fragments have been observed. IR spectroscopy was a good indicator of the presence of both functionalities in all products, namely, aromatic systems and carboxylate groups. The IR spectra obtained were dominated by broad C−O stretching vibrations of trifluoroacetate groups at 1660 and 1190 cm⁻¹ with distinctive bands of aromatic ligands also present: C−H stretching around 3050−2950 cm⁻¹ and in-plane vibrations of the C=C bonds in the 1600−1300 cm⁻¹ region (see Supporting Information).

The fundamentals of the synthetic experimental technique we applied have been presented elsewhere.[8] The ratio of components in the initial mixture, the temperature, and the duration of the sublimation−deposition procedures were the main variables in our experiments. In general, the combination of these factors represents complex multidimensional parameter systems whose exploration was pursued empirically. To synthesize the desired product we first investigated the relation between the experimental variables mentioned above and the appearance of the particular composition. The optimized experimental conditions for the synthesis of all adducts are summarized in Table 1.

The yields of all reactions studied were moderate. Typically, reactions were stopped after 3−5 days, affording 20−35% yields of crystalline products, although increasing the duration of reactions resulted in higher yields.

The optimal temperature regime for each system was the most important parameter. The selection of the initial temperature conditions was directly connected with the melting temperatures of PAHs: the higher the melting point, the higher the reaction temperature needed. The ligands suitable for our experiments

**Table 2.**  Crystallographic Data and Structure Refinement Details for $[Rh_2(O_2CCF_3)_4]_x(L)_y$ Adducts (**1−9**)

| | 1b | 2b | 3b | 4b | 5b | 6a | 6b′ |
|---|---|---|---|---|---|---|---|
| formula | $Rh_2O_8F_{12}C_{20}H_8$ | $Rh_2O_8F_{12}C_{20}H_{10}$ | $Rh_2O_8F_{12}C_{22}H_{10}$ | $Rh_2O_8F_{12}C_{22}H_{10}$ | $Rh_2O_8F_{12}C_{24}H_{10}$ | $Rh_2O_8F_{12}C_{40}H_{20}$ | $Rh_2O_8F_{12}C_{24}H_{10}$ |
| fw | 810.08 | 812.10 | 836.12 | 836.12 | 860.14 | 1062.38 | 860.14 |
| crystal system | monoclinic | monoclinic | triclinic | triclinic | monoclinic | triclinic | monoclinic |
| space group | $P2_1/n$ | $C2/c$ | $P\bar{1}$ | $P\bar{1}$ | $C2/m$ | $P\bar{1}$ | $P2_1/c$ |
| color of crystal | green | blue-green | green | dark green | dark green | green | green |
| $a$, Å | 11.287(7) | 22.562(3) | 8.480(2) | 8.642(1) | 9.317(2) | 8.674(3) | 9.2257(2) |
| $b$, Å | 17.509(4) | 8.577(1) | 8.6371(7) | 9.2100(7) | 14.902(1) | 9.464(2) | 9.224(1) |
| $c$, Å | 12.606(3) | 16.889(2) | 10.252(1) | 17.387(3) | 9.507(1) | 12.110(3) | 31.827(2) |
| $\alpha$, deg | | | 114.681(7) | 75.608(4) | | 77.91(2) | |
| $\beta$, deg | 93.64(3) | 131.34(2) | 99.736(7) | 85.458(8) | 103.45(1) | 76.65(1) | 93.97(5) |
| $\gamma$, deg | | | 98.147(7) | 81.362(5) | | 87.44(2) | |
| $V$, Å$^3$ | 2486(2) | 2453.8(5) | 653.3(2) | 1324.0(3) | 2751(1) | 956.2(5) | 2701.8(4) |
| $Z$ | 4 | 4 | 1 | 2 | 4 | 1 | 4 |
| temp (°C) | −60 | −60 | −60 | −60 | −60 | −60 | −60 |
| R1,$^b$ | 0.0671 | 0.0386 | 0.0458 | 0.0511 | 0.0588 | 0.0548 | 0.0440 |
| wR2$^c$ [$I > 2\sigma(I)$] | 0.1580 | 0.0893 | 0.1253 | 0.1455 | 0.1302 | 0.1532 | 0.1031 |
| R1,$^b$ | 0.0864 | 0.0419 | 0.0513 | 0.0547 | 0.0748 | 0.0584 | 0.0480 |
| wR2$^c$ (all data) | 0.1937 | 0.0923 | 0.1287 | 0.1530 | 0.1491 | 0.1590 | 0.1080 |
| GOF$^d$ | 1.085 | 1.129 | 1.100 | 1.076 | 1.086 | 1.067 | 1.085 |

| | 6b | 7b | 8a | 8c | 9b | 9c |
|---|---|---|---|---|---|---|
| formula | $Rh_2O_8F_{12}C_{24}H_{10}$ | $Rh_2O_8F_{12}C_{26}H_{12}$ | $Rh_2O_8F_{12}C_{44}H_{24}$ | $Rh_6O_{24}F_{36}C_{60}H_{24}$ | $Rh_2O_8F_{12}C_{26}H_{12}$ | $Rh_6O_{24}F_{36}C_{42}H_{12}$ |
| fw | 860.14 | 886.18 | 1114.45 | 2430.25 | 886.18 | 2201.98 |
| crystal system | monoclinic | triclinic | triclinic | triclinic | triclinic | triclinic |
| space group | $P2_1/c$ | $P\bar{1}$ | $P\bar{1}$ | $P\bar{1}$ | $P\bar{1}$ | $P\bar{1}$ |
| color of crystal | blue-green | green | dark green | light green | green | green |
| $a$, Å | 10.100(3) | 9.224(3) | 8.653(1) | 9.420(1) | 8.578(2) | 9.094(5) |
| $b$, Å | 17.535(3) | 10.546(3) | 9.2512(8) | 10.215(1) | 9.2958(7) | 12.277(3) |
| $c$, Å | 15.969(1) | 16.437(3) | 12.880(2) | 19.648(5) | 9.404(2) | 14.541(4) |
| $\alpha$, deg | | 89.78(3) | 80.292(5) | 94.99(2) | 98.62(4) | 77.02(2) |
| $\beta$, deg | 103.45(1) | 74.90(2) | 74.776(6) | 95.29(1) | 106.18(8) | 80.82(4) |
| $\gamma$, deg | | 75.03(2) | 88.113(6) | 95.05(1) | 97.91(2) | 79.86(3) |
| $V$, Å$^3$ | 2751(1) | 1487.9(7) | 980.6(2) | 1866.6(5) | 699.4(2) | 1545(1) |
| $Z$ | 4 | 2 | 1 | 1 | 1 | 1 |
| temp (°C) | −60 | −60 | −60 | −60 | −60 | −60 |
| R1,$^b$ | 0.0588 | 0.0634 | 0.0434 | 0.0866 | 0.0470 | 0.0721 |
| wR2$^c$ [$I > 2\sigma(I)$] | 0.1302 | 0.1455 | 0.0984 | 0.1666 | 0.1235 | 0.1596 |
| R1,$^b$ | 0.0748 | 0.0809 | 0.0500 | 0.1253 | 0.0527 | 0.0945 |
| wR2$^c$ (all data) | 0.1491 | 0.1654 | 0.1055 | 0.1965 | 0.1306 | 0.1851 |
| GOF$^d$ | 1.086 | 1.090 | 1.093 | 1.112 | 1.063 | 1.081 |

$^a$ Observation criteria $I > 2\sigma(I)$. $^b$ R1 = $\sum||F_o| - |F_c|/\sum|F_o|$. $^c$ wR2 = $[\sum[w(F_o^2 - F_c^2)^2]/\sum[w(F_o^2)^2]]^{1/2}$. $^d$ GOF = $[\sum[w(F_o^2 - F_c^2)^2]/(N_{observns} - N_{params})]^{1/2}$, based on all data.

all have melting points in the range 80−250 °C. The upper temperature limit is defined by the properties of the selected Lewis acid, $Rh_2(O_2CCF_3)_4$, which tends to deposit in its unligated form at temperatures above 200 °C. A clear illustration of this is provided by the work with series of isomers of the $C_{18}H_{12}$ composition: for the 2,3-benzanthracene having the highest melting temperature (>300 °C) no crystalline products have been isolated, in contrast to the outcomes with 1,2-benzanthracene (**L7**), triphenylene (**L8**), and chrysene (**L9**) (Table 1). For the same system, $Rh_2(O_2CCF_3)_4$-L, higher temperatures favor the products with the higher [Rh$_2$]:L ratio (**6b′** over **6a**, and **9c** over **9b**). Interestingly, two different types of crystals of the same composition 1:1 have been obtained for **L6** at distinctly different temperature regimes: low-temperature modification (100−105 °C) and high-temperature isomer (160 °C).

The ratio Rh$_2$ to L in the initial solid mixtures was typically close to 1:1 and varied in the range from 1:0.6 to 1:2. The slight excess of ligand favored the formation of bis-adducts **6a** and **8a**, while low concentrations of ligand resulted in better yields of **8c** and **9c**. The preferential composition of products obtained was 1:1 for all ligands, with only the exception of triphenylene (**L8**), for which all attempts to isolate a monoadduct were unsuccessful.

For **L6** and **L8** ligands a mixture of products (**6a**/**6b** and **8a**/**8c**, respectively) was formed in one reaction, but the crystals

were well separated by deposition in different parts of the ampules.

It is worth noting that the adduct **2b** was first found as a side-product of the reaction with acenaphthylene (**L1**). The ligand $C_{12}H_8$ purchased from Aldrich is known to contain up to 20% of acenaphthene (**L2**). Later **2b** was obtained in moderate yield from the direct reaction of $Rh_2(O_2CCF_3)_4$ with pure acenaphthene.

**Structural Description of the $[Rh_2(O_2CCF_3)_4]_x(L)_y$ Adducts.** The majority of ligands used in this work, namely, **L1−L5**, and **L7**, produce only one type of adduct having 1:1 stoichiometry, $[Rh_2(O_2CCF_3)_4](L)$. All of these products (**1b−5b**, and **7b**) exhibit a one-dimensional polymeric chain structure consisting of alternating PAH ligands and dirhodium tetra-(trifluoroacetate) complexes (Figure 1). These infinite chains of $\{[Rh_2(O_2CCF_3)_4](L)\}_\infty$ have no strong interchain contacts and run parallel to each other in the structure. Each ligand exhibits a bidentate-bridging coordination with two rhodium atoms attached to the opposite sides of the aromatic plane ("one up, one down" fashion). In the product structures aromatic ligands bridge the dirhodium units so that the ring planes are almost, but not exactly, perpendicular to the dimetal axis. In fact, all angles between the Rh−Rh vector and the plane of the ligand are greater than 90°, spanning the range 97.5−106.2° (Table 3). The coordination mode of the PAH in each member of this family of adducts is of the $\eta^2$ type, so that one rhodium atom
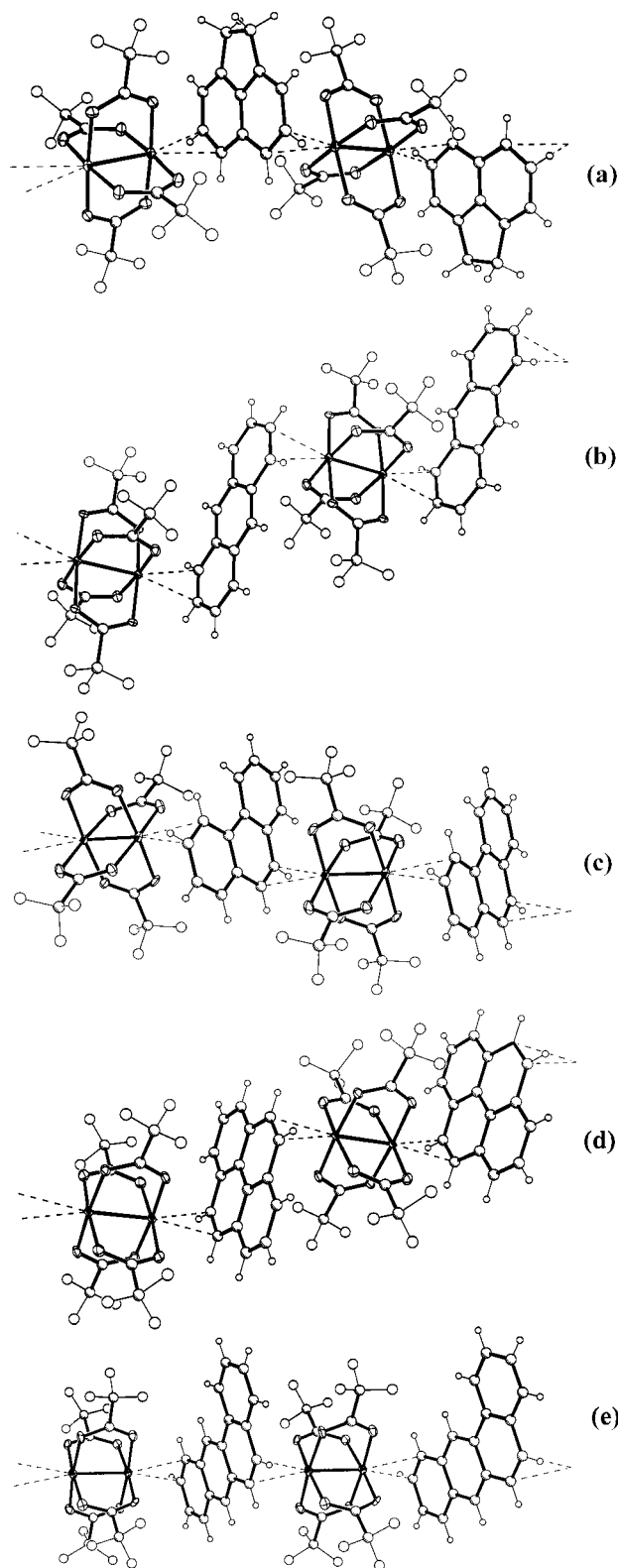
π-Electron Density in [Rh₂(O₂CCF₃)₄]x(L)y Adducts

*J. Am. Chem. Soc., Vol. 123, No. 47, 2001* 11659



**Figure 1.** Fragments showing the alternating arrangement of Rh₂(O₂CCF₃)₄ and polycyclic aromatic ligands in the 1D chain structures of monoadducts for (a) acenaphthene (**L2**); (b) anthracene (**L3**); (c) phenanthrene (**L4**); (d) pyrene (**L5**); (e) 1,2-benzathracene (**L7**). Rhodium and oxygen atoms are represented by thermal ellipsoids at the 40% probability level. Carbon, fluorine, and hydrogen atoms are shown as spheres of arbitrary radii. Only one orientation of the disordered CF₃ groups is depicted. The shortest Rh−C_arene contacts are drawn by dashed lines. Similar conventions pertain in subsequent figures.

is bound to two carbon atoms or to one C−C bond of the ligand but with inequivalent (except **5b**) and rather long Rh−C linkages. There are two sets (**1b**, **4b**, **7b**) or one set (**2b**, **3b**, **5b**) of Rh−C distances, depending on whether there is coordination of equivalent or inequivalent carbon−carbon bonds of the aromatic ligand.

Coordination of only "external" carbon atoms (i.e., those having H-atoms attached) is observed in all of these structures, **1b**−**5b** and **7b**. The Rh−Rh distances in the dirhodium complex span a narrow range of 2.425−2.431 Å; the Rh−Rh−C angles are 164.0−165.4°. The Rh−C contacts are in the range of 2.53−2.65 Å, except for the shortest distance of 2.47(1) Å which was observed in **1b** where there is a Rh atom attached to the 1,2-C≡C double bond of acenaphthylene (Figure 2). All coordinated carbon−carbon bonds of PAHs range from 1.30(1) to 1.38(1) Å, and the adjacent C−C−C angles are 120.9(6)−123.0(9)°; mean deviations from planarity for these ligands are 0.005−0.023 Å. This shows that no significant distortions of the aromatic systems are observed upon their coordination to rhodium compared to the structures of uncoordinated ligands.[11]

Fluoranthene (**L6**) was the first ligand affording two adducts with 1:1 and 1:2 ratios of Rh₂ to L. In addition, for a monoadduct composition, **L6** was the only ligand giving two coordination isomers, **6b** and **6b′**. Both have the same overall infinite chain structure {[Rh₂(O₂CCF₃)₄](C₁₆H₁₀)}∞ but differ by the ligand coordination mode to the rhodium centers (Figure 3).

In the low-temperature isomer **6b** the coordination of the ligand (Figure 3a) occurs through the 2,3- and the 6,12-positions of fluoranthene according to the numbering[12] in Schemes 2 and 3. This is the only case among all products in this work where an "internal" carbon atom (one connected with three other C atoms) is involved in coordination. This might be the reason this Rh−C contact in **6b** is the longest (2.735(6) Å) among all other 1:1 structures. Also in **6b** the inequivalence of the Rh−C distances is the most pronounced with Δ Rh−C being 0.072 and 0.128 Å for 2,3 and 6,12, respectively.

In the high-temperature isomer **6b′** (Figure 3b) fluoranthene also binds to the metal center through the same 2,3-position, but the second coordination involves just one carbon atom at the position 7 (Schemes 2 and 3). The Rh−C distance to this C atom is 2.582(7) Å, while contacts to two adjacent carbon atoms are longer than 2.9 Å; the Rh−Rh−C angle in this case is 172.6(2)°. This is the only example of an η¹ coordination among all the aromatic systems (and π-systems in general) that we have studied so far.

Fluoranthene (**L6**) also affords a 1:2 complex which has a typical bis-adduct type structure [Rh₂(O₂CCF₃)₄](C₁₆H₁₀)₂ (**6a**). It is a centrosymmetric molecule with a fluoranthene ligand axially bound at each end of the Rh₂(O₂CCF₃)₄ molecule (Figure 4). The shortest F···H intermolecular contacts between CF₃ groups and aromatic ligands are longer than 3.2 Å. The fluoranthene molecules in this structure are bound through the 2,3 carbon−carbon bond, as in the other fluoranthene compound. The Rh−C bonds in the bis-adduct (averaged to 2.574(5) Å) are a little bit shorter than those in structures **6b** and **6b′**, while the angle between the Rh−Rh direction and the aromatic plane of 112.8° is greater than for the chain structures. In addition,

(11) (a) Mason, R. *Acta Crystallogr.* **1964**, *17*, 547−555. (b) Welberry, T. R. *Proc. R. Soc. London A* **1973**, *334*, 19−48. (c) Ahmed, F. R.; Trotter, J. *Acta Crystallogr.* **1963**, *16*, 503−508. (d) Ferraris, G.; Jones, D. W.; Yerkess, J. *Z. Kristallogr.* **1973**, *138*, 113−128. (e) Hazell, A. C.; Jones, D. W.; Sowden, J. M. *Acta Crystallogr.* **1977**, *B33*, 1516−1522.

(12) Fox, R. B.; Powell, W. H. *Nomenclature of Organic Compounds, Principles and Practice*, 2nd ed.; Oxford, University Press: New York, 2001; pp 79−82.

**Table 3.** Selected Distances (Å) and Angles (deg) in Adducts [Rh$_2$(O$_2$CCF$_3$)$_4$]$_x$(L)$_y$.

| No. | ligand | Rh$_2$:L | Rh−Rh | Rh···C | C−C | Rh−Rh···C (av) | C−C−C$^a$ (av) | mean dev.$^b$ | Rh−Rh/plane$^c$ |
|---|---|---|---|---|---|---|---|---|---|
| **1b** | L1 | 1:1 | 2.430(2) | 2.65(1), 2.66(1) | 1.37(2) | 165.0(2) | 121(1) | 0.016 | 106.2 |
| | | | | 2.47(1), 2.53(1) | 1.38(1) | 164.0(2) | 108.2(9) | | 97.9 |
| **2b** | L2 | 1:1 | 2.429(1) | 2.599(6), 2.647(6)$^d$ | 1.377(9) | 164.8(1) | 120.9(6) | 0.023 | 97.5 |
| **3b** | L3 | 1:1 | 2.4294(8) | 2.574(6), 2.603(5)$^d$ | 1.360(9) | 164.8(2) | 121.1(6) | 0.016 | 100.1 |
| **4b** | L4 | 1:1 | 2.4254(6) | 2.615(6), 2.627(6) | 1.35(1) | 164.8(2) | 121.2(6) | 0.014 | 102.4 |
| | | | | 2.556(5), 2.563(6) | 1.30(1) | 165.3(2) | 121.9(6) | | |
| **5b** | L5 | 1:1 | 2.4304(7) | 2.578(3)$^e$ | 1.336(8) | 164.92(9) | 121.5(2) | 0.005 | 97.7 |
| **7b** | L7 | 1:1 | 2.431(1) | 2.528(9), 2.53(1) | 1.31(2) | 165.0(2) | 123.0(9) | 0.013 | 103.1 |
| | | | | 2.60(1), 2.606(9) | 1.32(2) | 165.4(2) | 121.8(9) | | |
| **6b** | L6 | 1:1 | 2.423(1) | 2.598(6), 2.672(6) | 1.38(1) | 164.8(2) | 121.1(6) | 0.054 | 98.5 |
| | | | | 2.607(6), 2.735(6) | 1.35(1) | 165.0(1) | 118.1(6) | | |
| **6b′** | L6 | 1:1 | 2.4255(9) | 2.582(7)$^f$ | 1.38(1) | 172.6(2) | 119.8(7) | 0.058 | 99.9 |
| | | | | 2.571(8), 2.618(8) | 1.37(1) | 164.7(2) | 121.8(7) | | |
| **9b** | L9 | 1:1 | 2.427(1) | 2.573(6), 2.601(6)$^d$ | 1.32(1) | 165.2(2) | 122.3(6) | 0.009 | 103.7 |
| **6a** | L6 | 1:2 | 2.4257(9) | 2.554(5), 2.594(5)$^d$ | 1.378(9) | 163.9(2) | 121.4(5) | 0.040 | 112.8 |
| **8a** | L8 | 1:2 | 2.4245(8) | 2.564(5), 2.707(5)$^d$ | 1.376(8) | 163.9(1) | 120.8(5) | 0.037 | 118.3 |
| **8c** | L8 | 3:2 | 2.422(2) | 2.56(2), 2.72(2) | 1.38(2) | 164.6(4) | 121(2) | 0.082 | 102.7 |
| | | | 2.416(3) | 2.58(2), 2.73(2) | 1.37(2) | 165.1(4) | 121(2) | | 118.4 |
| | | | | 2.59(2), 2.68(2)$^d$ | 1.36(2) | 164.8(4) | 121(2) | | |
| **9c** | L9 | 3:1 | | 2.327(9)$^g$ | | 169.9(2)$^h$ | | | |
| | | | 2.404(2) | 2.52(1), 2.62(1) | 1.35(2) | 164.5(3) | 122(1) | 0.018 | 103.0 |
| | | | 2.421(2) | 2.51(1), 2.61(1)$^d$ | 1.35(2) | 164.7(3) | 121(1) | | 102.3 |

$^a$ Angles adjacent to coordinated C−C bond. $^b$ Mean deviation from the plane (Å) for coordinated ligand. $^c$ The angle between Rh−Rh vector and aromatic plane (deg). $^d$ The second set of Rh···C distances is the same. $^e$ All four Rh···C distances are the same. $^f$ $\eta^1$-coordination. $^g$ Rh−O$_{carboxyl}$ axial contact. $^h$ Rh−Rh−O$_{carboxyl}$ angle.
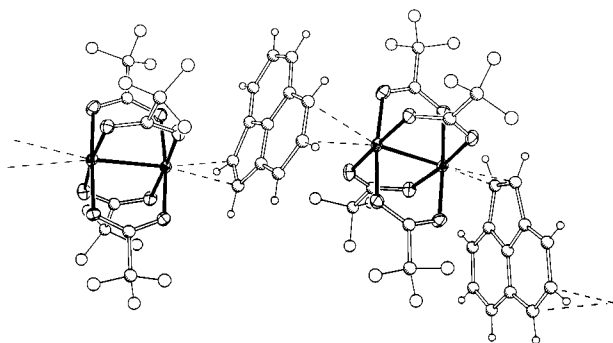


**Figure 2.** A fragment of the 1D chain structure with acenaphthylene (**L1**), {Rh$_2$(O$_2$CCF$_3$)$_4$·(C$_{12}$H$_8$)}$_\infty$ (**1b**).



(a)



(b)
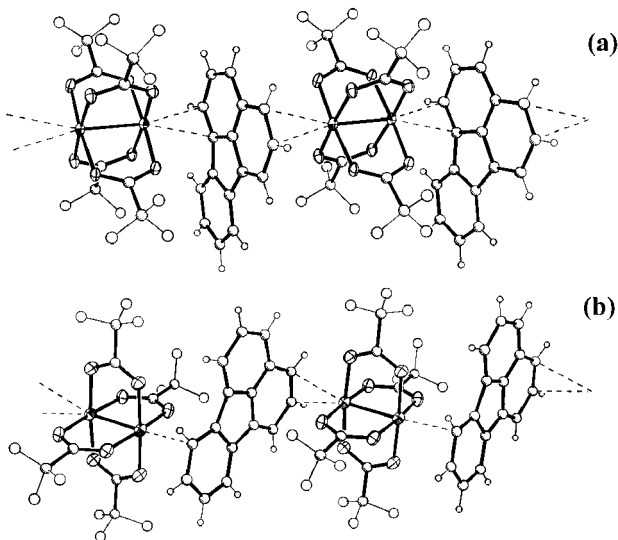
**Figure 3.** Fragments of the 1D coordination polymers with fluoranthene (**L6**), [Rh$_2$(O$_2$CCF$_3$)$_4$]·(C$_{16}$H$_{10}$) (a) **6b**; (b) **6b′**.

**L6** exhibits high mean deviations from planarity: 0.054, 0.058, and 0.040 Å, for **6b**, **6bN**, and **6a**, respectively.

Triphenylene (**L8**) was the only ligand studied here which does not produce a 1:1 type of product under any experimental

**Scheme 3**
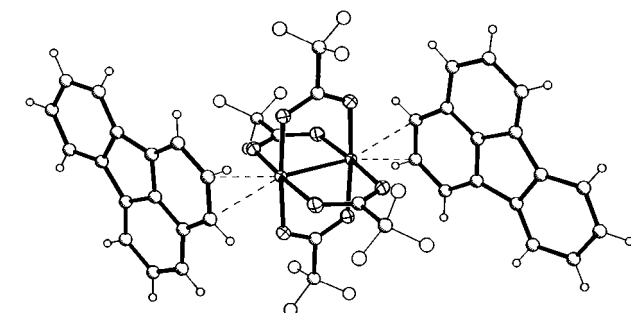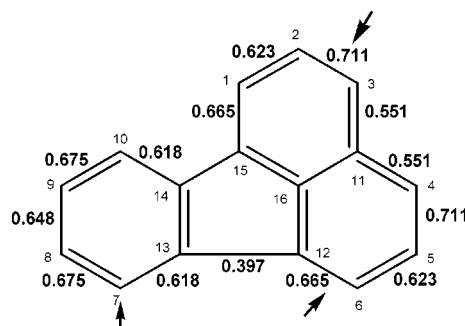




**Figure 4.** A perspective drawing of the bis-adduct molecule with fluoranthene (**L6**), [Rh$_2$(O$_2$CCF$_3$)$_4$]·(C$_{16}$H$_{10}$)$_2$ (**6a**).

conditions tested. However, two other stoichiometries have been found for **L8**, namely the 1:2 and 3:2. In the bis-adduct [Rh$_2$(O$_2$CCF$_3$)$_4$](C$_{18}$H$_{12}$)$_2$ (**8a**) coordination of the ligand (similar to the one observed in **6a**) through only one C−C bond with unequal Rh−C distances Δ = 0.14 Å was observed (Figure 5). This coordination was accompanied by the highest angle, 118.3°, between the Rh−Rh direction and the aromatic plane of the ligand found in any of these compounds.

The remarkable structure of the 3:2 adduct with triphenylene, [Rh$_2$(O$_2$CCF$_3$)$_4$]$_3$(C$_{16}$H$_{10}$)$_2$ (**8c**) is shown in Figure 6. Each ligand exhibits a tridentate-bridging coordination using all three of the C−C bonds of the type used in **8a**, each from a different aromatic ring. That gives a ribbon-type structure in which
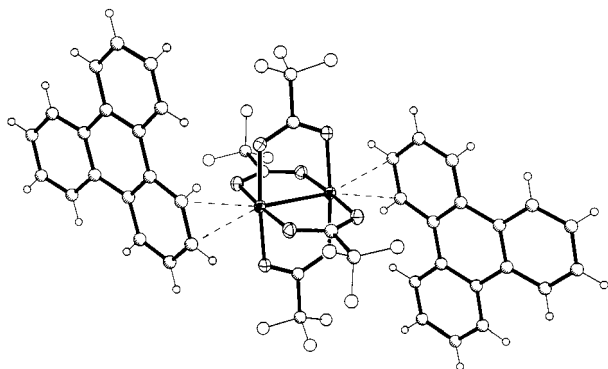
**Figure 5.** A perspective drawing of the bis-adduct molecule with triphenylene (**L8**), [Rh$_2$(O$_2$CCF$_3$)$_4$]·(C$_{18}$H$_{12}$)$_2$ (**8a**).
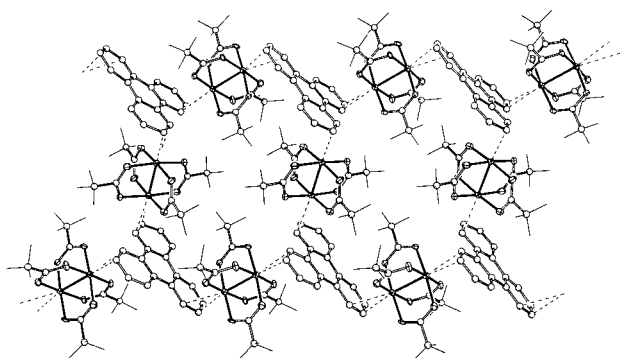


**Figure 6.** The pseudo-2D ribbon-type structure with triphenylene (**L8**), {[Rh$_2$(O$_2$CCF$_3$)$_4$]$_3$·(C$_{18}$H$_{12}$)$_2$} (**8c**). Hydrogen atoms and fluorine atoms of CF$_3$ groups are omitted for clarity.

formally two infinite chains of monoadducts are stapled together by additional Rh$_2$(O$_2$CCF$_3$)$_4$ units. It is a pseudo-2D structure, in which an elemental unit can be considered as an octagon formed by four dirhodium complexes and four triphenylene ligands. All of these octagons are conjugated through aromatic ligands to form ribbons which lie parallel in the crystal. The shortest contacts between two different ribbons, F···H, are all longer than 2.5 Å. There are two crystallographically independent dirhodium units in the structure **8c**. One of these forms 1:1 infinite chains running horizontally at the top and bottom of Figure 6. The other one, which staples these chains together, coordinates to the equivalent C—C bonds and has an inversion center in the middle of the Rh—Rh bond. Each ligand can be considered to have "two up, one down" coordination, which is probably the reason the highest mean deviation from planarity (0.082 Å) for the PAH occurs in this structure. For each coordinated C—C bond the Rh—C distances are inequivalent with differences of 0.16, 0.15, and 0.09 Å. The structure of **8c** is reminiscent of the structure of [Rh$_2$(O$_2$CCF$_3$)$_4$]$_3$(S$_8$)$_2$ prepared by us recently[8g] where the eight-membered sulfur rings also were functioning in a tridentate-bridging fashion to form a ribbon.

Chrysene (**L9**) also gives two adducts, with 1:1 and 3:1 compositions. The compound {[Rh$_2$(O$_2$CCF$_3$)$_4$](C$_{18}$H$_{12}$)}$_\infty$ (**9b**) has a typical structure for 1:1 adducts, which is very similar to that of the naphthalene 1D polymer.[8f] Rhodium atoms of Rh$_2$(O$_2$CCF$_3$)$_4$ in **9b** bind to the equivalent carbon—carbon bonds of the inner aromatic rings of **L9** (Figure 7).

Compound **9c** with a 3:1 composition is particularly interesting as the first real 2D network in this class of adducts. Each chrysene molecule acts in a tetradentate mode, bridging to four metal centers of four different dirhodium complexes, two on each side of the aromatic plane. Two C—C bonds on each of
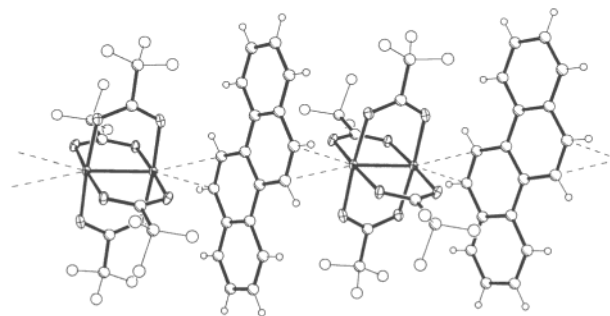


**Figure 7.** A fragment showing the alternating arrangement of Rh$_2$(O$_2$CCF$_3$)$_4$ and chrysene ligands (**L9**) in the chain structure of {[Rh$_2$(O$_2$CCF$_3$)$_4$]·(C$_{18}$H$_{12}$)}$_\infty$ (**9b**).
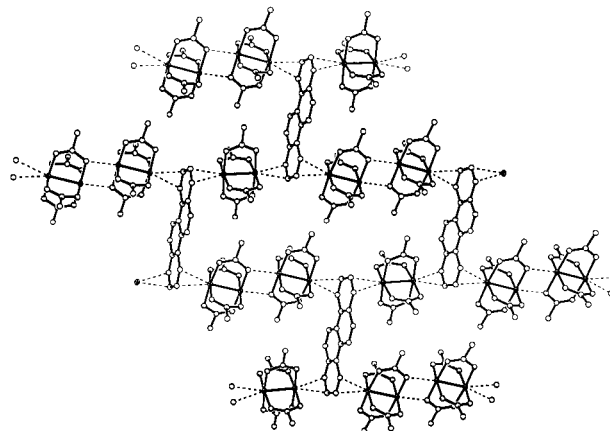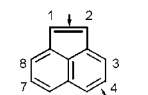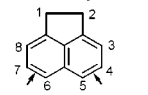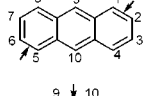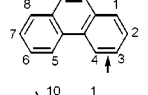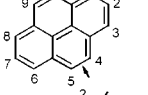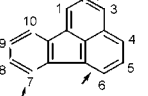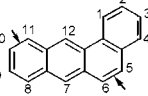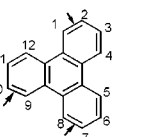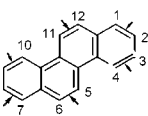


**Figure 8.** The 2D network with chrysene ligands (**L9**), {[Rh$_2$(O$_2$CCF$_3$)$_4$]$_3$·(C$_{18}$H$_{12}$)}$^2_\infty$ (**9c**). Hydrogen and fluorine atoms of CF$_3$ groups are omitted for clarity.

the outer aromatic rings of chrysene are used in the "up-and-down" fashion. This is the only case where aromatic bonds involved in coordination are separated just by one C—C bond in the ligand, and all four of these bonds in **9c** are different from those employed in **9b** for bidentate binding to the rhodium centers. The structure of **9c** consists of the layers shown in Figure 8 separated by the parameter $a$ of the unit cell (9.094(5) Å). Actually, for such a coordination mode of chrysene the Rh$_2$:L ratio of 2:1 would be enough to create such a layered motif. In fact, in structure **9c** only one dirhodium unit binds to two aromatic ligands. Two other dirhodium complexes axially bind only one aromatic ligand each, and they are linked together on their other ends through mutual axial coordination of carboxylic oxygen atoms. The Rh···O distances for such coordination (2.372(9) Å) are much shorter than for the Rh—C bonds which average to 2.57(1) Å. The aromatic planes of **L9** are perpendicular to the plane of the adduct layer, with other layers in the structure being located parallel but shifted slightly so that the chrysene ligands are not exactly over each other. This leads to the shortest interlayer contacts of 2.32 Å between fluorine atoms of CF$_3$ groups and hydrogen atoms of the chrysene molecules.

## Discussion

The employment in this work of the $π$-electrons of polycyclic aromatic hydrocarbons as donors and dimetal units in the form of dirhodium(II) tetra(trifluoroacetate) complexes as acceptors is an unprecedented approach to generating novel extended donor—acceptor networks. The potential of PAHs with their varied shapes and properties for building macromolecules and forming supramolecules with transition metal centers has been

**Table 4.** Comparison of Coordination of Modes of PAHs in Adducts **1**−**9** with $\pi$-Electron Density Distribution in Ligands (**L1**−**L9**)

| Ligand | HMO (selected C-C bonds) | | Product | Type of adduct | Bridging mode |
|---|---|---|---|---|---|
| **L1** acenaphthylene $C_{12}H_8$ | 1-2<br>4-5, 6-7<br>3-4, 7-8 | 0.795<br>0.703<br>0.632 | **1b** | 1:1 | $\mu^2 - \eta^2(1,2) : \eta^2(4,5)$ |
| **L2** acenapthene $C_{12}H_{10}$ | 4-5, 6-7<br>3-4, 7-8 | 0.724<br>0.602 | **2b** | 1:1 | $\mu^2 - \eta^2(4,5) : \eta^2(6,7)$ |
| **L3** anthracene $C_{14}H_{10}$ | 1-2, 5-6<br>2-3, 6-7 | 0.7 37<br>0.585 | **3b** | 1:1 | $\mu^2 - \eta^2(1,2) : \eta^2(5,6)$ |
| **L4** phenanthrene $C_{14}H_{10}$ | 2-3, 6-7<br>3-4, 5-6<br>9-10 | 0.707<br>0.702<br>0.775 | **4b** | 1:1 | $\mu^2 - \eta^2(3,4) : \eta^2(9,10)$ |
| **L5** pyrene $C_{16}H_{10}$ | 1-2, 2-3<br>4-5, 9-10 | 0.669<br>0.776 | **5b** | 1:1 | $\mu^2 - \eta^2(4,5) : \eta^2(9,10)$ |
| **L6** fluoranthene $C_{16}H_{10}$ | 1-2, 6-5<br>2-3, 4-5<br>7-8, 9-10<br>1-15, 6-12 | 0.623<br>0.711<br>0.675<br>0.665 | **6a**<br>**6b**<br>**6b'** | 1:2<br>1:1<br>1:1 | $\eta^2(2,3)$<br>$\mu^2 - \eta^2(2,3) : \eta^2(6,12)$<br>$\mu^2 - \eta^2(2,3) : \eta^1(7)$ |
| **L7** 1,2-benzanthracene $C_{18}H_{12}$ | 3-4<br>5-6<br>8-9<br>10-11 | 0.700<br>0.783<br>0.731<br>0.730 | **7b** | 1:1 | $\mu^2 - \eta^2(5,6) : \eta^2(10,11)$ |
| **L8** triphenylene $C_{18}H_{12}$ | 1-2, 3-4<br>2-3 | 0.690<br>0.636 | **8a**<br>**8c** | 1:2<br>3:2 | $\eta^2(1,2)$<br>$\mu^3 - \eta^2(1,2) : \eta^2(7,8) :$ $\eta^2(9,10)$ |
| **L9** chrysene $C_{18}H_{12}$ | 1-2, 7-8<br>2-3, 8-9<br>3-4, 9-10<br>5-6, 11-12 | 0.712<br>0.617<br>0.707<br>0.754 | **9b**<br>**9c** | 1:1<br>3:1 | $\mu^2 - \eta^2(5,6) : \eta^2(11,12)$<br>$\mu^4 - \eta^2(1,2) : \eta^2(3,4) :$ $\eta^2(7,8) : \eta^2(9,10)$ |

largely neglected. Only the organometallic chemistry of Ag$^+$ with a variety of aromatic ligands has been explored in solutions.[13] In contrast to the interaction of a single metal center with PAH systems, the use of a bifunctional dinuclear transition metal unit in the supramolecular design allows the creation of much more elaborate structures. These structures cover a range of stoichiometries but yet have some common features.

Presently, the HMO model is considered to be largely of historical interest in the development of quantum chemistry. However, because of its extreme simplicity, especially when implemented by an efficient computer program,[14] we were interested in how well the results of Hückel calculations would correlate with the molecular structures of the products.

In our earlier report[8f] of the chain structure of the 1:1 naphthalene adduct we noted that, of the four types of C−C

(13) (a) Griffith, E. A. H.; Amma, E. L. *J. Am. Chem. Soc.* **1974**, *96*, 5409−5413. (b) Ning, G. L.; Wu, L. P.; Sugimoto, K.; Munakata, M.; Suenaga, Y.; Kuroda-Sowa, T.; Maekawa, M. *J. Chem. Soc., Dalton Trans.* **1999**, 2529−2536. (c) Munakata, M.; Ning, G. L.; Suenaga, Y.; Sugimoto, K.; Kuroda-Sowa, T.; Maekawa, M. *Chem. Commun.* **1999**, 1545−1546. (d) Munakata, M.; Wu, L. P.; Ning, G. L.; Kuroda-Sowa, T.; Maekawa, M.; Suenaga, Y.; Maeno, N. *J. Am. Chem. Soc.* **1999**, *121*, 4968−4976. (e) Ino, I.; Wu, L. P.; Munakata M.; Kuroda-Sowa, T.; Maekawa, M.; Suenaga, Y.; Sakai, R. *Inorg. Chem.* **2000**, *39*, 5430−5436. (f) Munakata, M.; Wu, L. P.; Ning, G. L. *Coord. Chem. Rev.* **2000**, *198*, 171−203.

(14) Wissner, A. *HMO plus 2.8.3*; Wyeth-Ayerst Research, Le Derte Laboratories: Pearl River, NY 10965, 1989, 1992−1995.

bonds potentially available as coordination sites, the two involved in bonding were the type that, according to Hückel theory, have the greatest $\pi$-electron density. Therefore, in addition to our general interest in the types of structures that could be obtained with $Rh_2(O_2CCF_3)_4$ and polycyclic aromatic systems, we were curious as to how faithfully the binding sites at other, and larger, molecules would be predicted by Hückel HMO calculations.

The electronic effect observed in the naphthalene polymer[8f] is even more pronounced for the related ligand examined here, acenaphthylene (**L1**). Hückel calculations for **L1** confirmed that the highest $\pi$-bond order (0.795) is in the double carbon−carbon bond (1−2) in the five membered ring, with the 4−5 bond in the naphthalene part of the molecule having the second highest (0.703). Indeed, in the 1D polymer **1b** (Figure 2) it is just these two C−C bonds that are engaged in coordination to the Rh centers of dirhodium tetra(trifluoroacetate).

For all of the structures reported here, the actual points of attachment of rhodium atoms to the PAHs are compared with the $\pi$-electron density distribution in Table 4. In general the correlation between points of attachment and calculated $\pi$-density maxima is good, but a number of individual cases deserve discussion.

For acenaphthene (**L2**) the compound **2b** shows that, as might certainly have been expected, it is two bonds corresponding to

those previously observed in naphthalene itself[8f] that are coordinated (Figure 1a). For anthracene (**L3**) in **3b**, it is again two of the most electron-rich C−C bonds that bind to rhodium atoms (Figure 1b). In all of these cases, it could hardly be argued that the choice is based on steric factors; it is clearly a question of electronic structure.

For phenanthrene (**L4**), in compound **4b** (Figure 1c), of the two C−C bonds that are used, one is by far the most electron-rich, while the other is only one of the third-most, but this one is only slightly (0.702 vs 0.707) less rich than the second.

For both pyrene (**L5**) and triphenylene (**L8**), because of their high symmetries, there are only two kinds of external (as previously defined) C−C bonds. For both of these, compound **5b** for pyrene (Figure 1d) and compounds **8a** and **8c** for triphenylene (Figures 5 and 6), it is the bonds of the highest π-density to which the rhodium atoms are attached.

For chrysene (**L9**) there are four types of exterior C−C bonds, of which three types (two of each) are used for binding the rhodium atoms in complexes **9b** and **9c** (Figures 7 and 8). These are just the three types, six in all, with the highest π-electron densities.

For 1,2-benzanthracene (**L7**) in compound **7b**, after the 5−6 bond, which is the most electron-rich, the next two candidates, 8−9 and 10−11, differ insignificantly. The 10−11 bond is the one used in the construction of the 1D polymer (Figure 1e).

Fluoranthene (**L6**) is the odd actor in this case of characters, but perhaps that is not surprising. It really consists of a benzene ring attached (not fused) to a naphthalene molecule, with (as shown in Scheme 3) little mixing of the two sets of π-orbitals. It should be noted that the conventional representation of this molecule, which we have used here, tends to obscure its symmetry ($C_{2v}$). In all of the compounds made with fluoranthene, **6a**, **6b**, and **6b′**, one of the bonds used, the 2−3 (equivalent to the 4−5), for binding a rhodium atom corresponds to the 1−2 bond in naphthalene, and has the highest π-density. In **6a**, this is the only point of attachment (Figure 4). The other two points of attachment in **6b** and **6b′** (Figure 3) are anomalous. The 6−12 bond, used in **6b**, is not between two exterior atoms although it has the third highest π-bond order. In fact this attachment is very unsymmetrical. Then, in **6b′**, in addition to attachment at the 2−3 bond, there is a weak coordination that is mainly to a single carbon atom, C7. This is the only example of such a situation among the compounds reported here or any others.

It is a remarkable result of this work that despite the apparent shortcomings of the HMO theory compared to the very sophisticated quantum chemical methods now available, the experimental results obtained are in excellent accord with the Hückel results. As we have noted, the rhodium-to-carbon distances are rather long, meaning that the interactions are relatively weak. Thus, the π-electron density distribution of the PAH is probed gently and is not likely to be changed by the probe itself. We therefore conclude that the results of HMO calculations of π-electron density do, at least qualitatively, reflect reality. We know of no other experimental study that provides comparable results.

The present findings may represent an alternative approach for synthesis of structurally diverse organometallic multidimensional materials. Numerous aromatic ligands with various coordination geometries may provide a wide range of possibilities for connecting dinuclear (and, prospectively, polynuclear) metal units together to construct many other supramolecular architectures. As only planar π-systems have been tested thus far, the resulting products had only 1D or 2D architectures. The use of nonplanar or branched PAH ligands would lead to 3D assemblies. Further investigations in this area of chemistry including different polynuclear metal complexes and a broader range of aromatic ligands are clearly warranted.